JOURNAL OF OPTOELECTRONICS AND ADVANCED MATERIALS Vol. 9, No. 8, August 2007, p. 2312 - 2316

Analysis of square-structured photonic crystal fibers using localized orthogonal function algorithm

XIAOLING TAN*, JIANQUAN YAO, YOUFU GENG, HUIYUN ZHANG, YUPING ZHANG, PENG WANG
College of Precision Instrument and Optoelectronics Engineering, Institute of Laser and Optoelectronics, Tianjin University, Tianjin 300072, China
Key Laboratory of Optoelectric Information Science and Technology of EOM. Tianjin University, Tianjin 300072, China

A modified localized orthogonal function method is applied to the analysis of square-structured PCFs. Because of difficulty in solving the vector wave equation, a scalar approximation is adopted. Then endlessly single-mode operation, electric field distribution, effective area and chromatic dispersion property are, respectively, evaluated. It is shown that the results agree well with the published data for the investigated wavelength window.

(Received December 7, 2006; accepted June 15, 2007)

Keywords: Photonic crystal fiber, Localized orthogonal function, Effective area

1. Introduction

Photonic crystal fibers (PCFs) consisting of a central defect region surrounded by air holes that run along the fiber length are attracting much attention in recent years because of unique properties which are not realized in conventional optical fibers, such as endlessly single-mode at all wavelengths [1], tailorable effective modal areas [2], anomalous dispersion at visible and near infrared band [3] and highly birefringent effect [4,5] etc. According to the guiding property, PCFs can be divided into two general classes. One class is photonic bandgap fiber [6,7], which transversely confines light in the defect core. The second class of PCFs is analogous to conventional index guiding fibers, and relies on a form of total internal reflection (TIR) [1, 8]. Numerical simulation plays an important role for the design and modeling of PCFs. So far, several modeling methods have been developed such as effective index approach [1], plane-wave expansion method (PWE) [9,10], localized orthogonal function method [11,12], finite-difference time-domain method (FDTD) [13], multipole method [14,15], beam propagation method(BPM) [16], finite-element method (FEM) [17] and so on.

In this paper a localized orthogonal function method is used to numerically simulate square-structured photonic crystal fibers. The transverse electromagnetic field is expanded by cosine functions, and the propagation constant could be calculated by recasting the Maxwell equation into an algebraic eigenvalue equation. Then we studied the principle parameters of the PCFs such as endlessly single mode operation, electric field distribution, effective area and chromatic dispersion property etc. which supplied a theoretical support for designing photonic crystal fibers with certain waveguide modes and dispersion properties.

2. Analysis method

The cross section of a PCF is schematically shown in Fig. 1, where a missing air hole forms the fiber core. d is the diameter of an air hole, and A is the hole-to-hole spacing or lattice pitch.

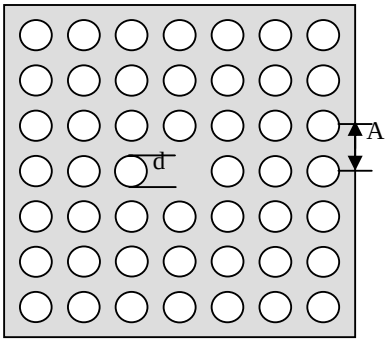

Fig.1. Schematic of a square-structured PCF.

The guided modes propagate along the fiber (z direction), so the electric field of the guided mode can be written as

$$\vec{E}(x,y,z) = [\vec{E}_t(x,y) + \vec{E}_z(x,y)]e^{i\beta z} \quad (1)$$

Where β is the propagation constant of the mode, E_t and E_z are the transverse and longitudinal components of the modal electric field respectively. Substituting Eq(1) into the wave equation, we get the equation for E_t

$$(\nabla_t^2 - \beta^2 + k^2 n^2)E_t = 0 \quad (2)$$

Where $k=2\pi/\lambda$ is the wave vector in free space; $n=n(x, y)$ the transverse refractive index profile.

To solve the equation (2), we expand electric field in terms of orthogonal function. Because the distribution of electric field is symmetrical, the cosine function is chosen as the basic function, while in [11, 12] the Hermite-Gaussian functions as the basic function, so the electric fields can be written as

$$E_t(x,y)=\sum_{a,b=1}^{N} c_{ab}\Phi_{ab}(x,y) \tag{3}$$

where $\Phi_{ab}(x,y)=\sqrt{\frac{4}{L_x L_y}}\cos(\pi ax/L_x)\cos(\pi bx/L_y)$;

N is the expansion order; c_{ab} is the expansion coefficient; L_x and L_y are the spatial dimensions.

Substituting Eq(3) into Eq (2) yields an algebraic eigenvalue equation

$$M\hat{V}=\frac{\beta^2}{k^2}\hat{V}=n_{eff}^2\hat{V} \tag{4}$$

Where

$$M_{abcd}=\frac{1}{k^2}I_{abcd}^{(1)}+I_{abcd}^{(2)}$$

$$I_{abcd}^{(1)}=-\pi^2\left(\frac{a^2}{L_x^2}+\frac{b^2}{L_y^2}\right)\delta_{ac}\delta_{bd}$$

$$I_{abcd}^{(2)}=\int_0^{L_x}\int_0^{L_y}\{n^2(x,y)\phi_{ab}(x,y)\phi_{cd}(x,y)\}dxdy$$

Solving the eigenvalue equation, the propagation constant and modal fields of guided modes can be obtained.

3. Simulation results and discussion

In the process of numerical simulation, considering the symmetry of the electric fields, one quadrant of the cross section is calculated, which is therefore very efficient and results in a considerable reduction of required memory space and CPU time.

The following two points also should be noticed:

(1) The expansion order should not be less than 14. Certainly the greater the order is, the more accurate the result is, but the calculation time will increase as the order' biquadratic, therefore the expansion order should be chosen properly.

(2) Because the PCFs we discussed here rely on a form of total internal reflection to guide light and the electric field mostly distributes in the fiber core, so only the air holes within seven or ten layers near the fiber core are calculated.

Using the method described above the simulation results are obtained as follows:

3.1. The endlessly single-mode operation

Conditions for single-mode operation of PCFs turn out to be very different from conventional fiber.With relative hole diameters (d/A) less than 0.45 [18], PCFs can be endlessly single-mode and even for large air holes single-mode operation is possible for wavelengths above a cutoff wavelength. A "phase" diagram is shown as Fig. 2. The solid line defines a "phase" boundary; above the line the PCF is single-mode and below it is multi-mode, and when d/A<0.45, there is an endlessly single-mode regime.

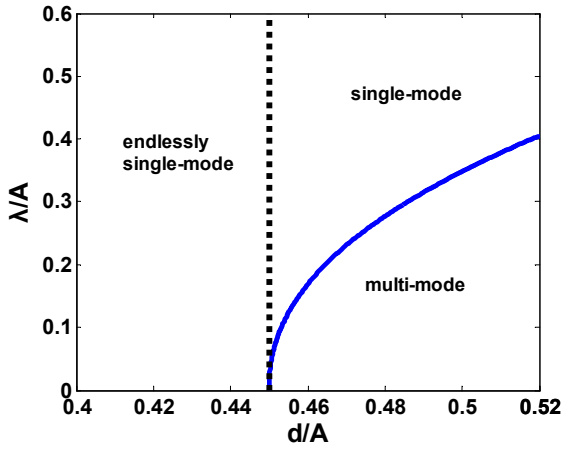

Fig. 2. Diagram illustrating "phase" with single-mode and multi-mode operation.

3.2. The electric field distribution

In a TIR PCF, the core index n_{co} is greater than the cladding index n_{cl} because of air holes, so the fiber can guide the light by total internal reflection as a standard fiber does. Fig. 3 plots the transverse electric field distribution of the fundamental mode in a PCF, where A=2.3 μm, d=0.46 μm, the background index of silica is assumed to be 1.444, and the operating wavelength is 1550 nm. Fig. 4 and Fig. 5 plot the transverse electric field distributions with the parameters A=2.3 μm, d=0.8 μm at λ=1550 nm and λ=900 nm respectively.

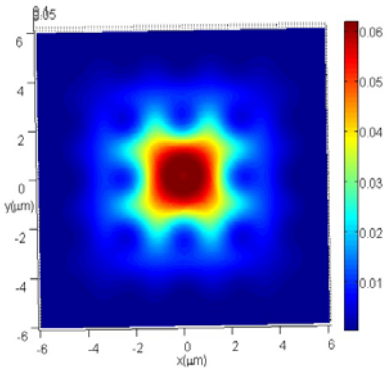

a

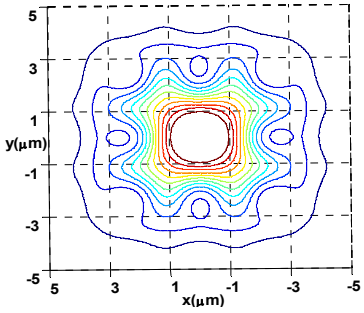

b

Fig. 3. The contour line of electric field distribution for the fundamental mode (A=2.3μm, d=0.46 μm, λ=1550 nm).

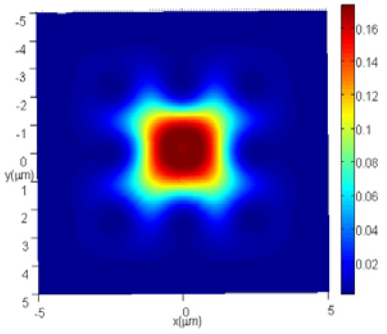

a

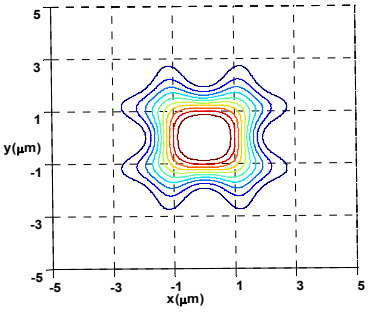

b

Fig. 4. The contour line of electric field distribution for the fundamental mode (A=2.3μm, d=0.8 μm, λ=1550 nm).

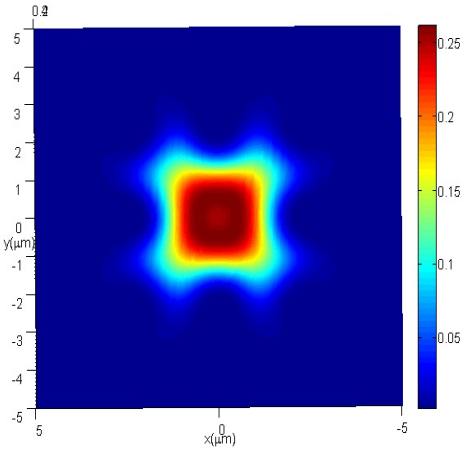

a

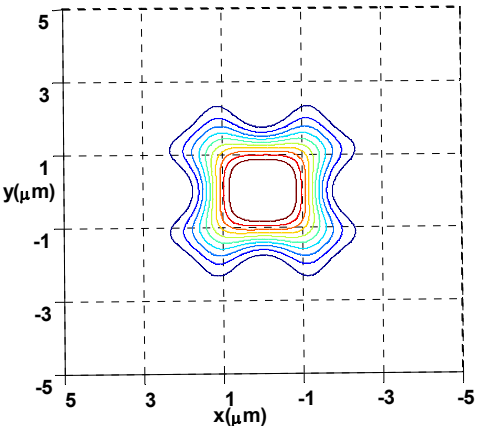

b

Fig. 5. The contour line of electric field distribution for the fundamental mode (A=2.3μm, d=0.8μm, λ=900 nm).

From the three figures above, it can be seen that the modal field is well confined within the core region. With larger air holes, the field is more concentrated in the fiber core, and the peak intensity appears greater. At the shorter wavelength the electric field does not extend into the air hole, contrarily to what occurs at the longer one, and the longer the wavelength is, the greater the expansion of the field into the air hole is.

3.3. The effective area

The area of the fundamental mode is clearly related to the effective area of the fiber core, A_{eff} is defined as [19]

$$A_{eff} = \frac{(\int_{-\infty}^{\infty}\int_{-\infty}^{\infty}|E_t|^2 dxdy)^2}{\int_{-\infty}^{\infty}\int_{-\infty}^{\infty}|E_t|^4 dxdy} \quad (5)$$

where E_t is the transverse electric field vector. Fig. 6 shows the effective area as a function of wavelength with different structure parameters. We can see that the effective area at higher wavelength is larger than that at shorter wavelength. Increasing the air-hole size or decreasing the hole-to-hole spacing, the mode becomes confined, and thus the effective area is reduced.

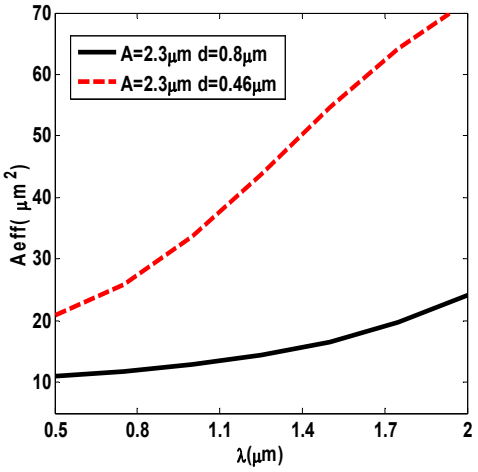

a

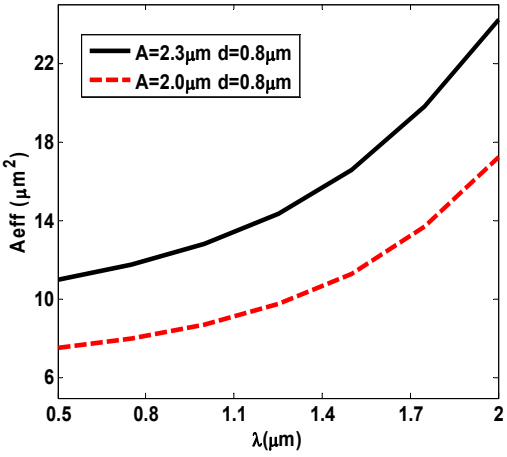

b

Fig. 6. The effective areas of PCF for (a) A=2.3 μm, (b) d=0.8 μm.

The effective area values of the square-structured PCFs are higher than those of the triangular PCFs with the same parameters in all wavelengths as shown in Fig. 7. The differences in the square-structured PCFs are with a lower air filling fraction ($f=(\pi/4)(d/A)^2$) than those of the triangular PCFs ($f=(\pi/2\sqrt{3})(d/A)^2$) [20]. As a result, the cladding index of the square-structured PCFs is higher which results in a higher effective area. The large mode area PCFs and high nonlinearity of PCFs can be designed and realized by changing the structure of PCFs.

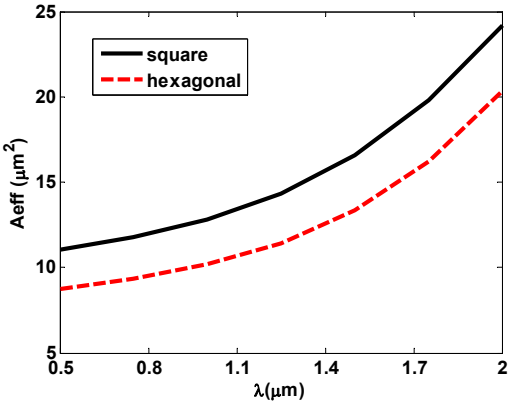

Fig. 7. Effective area comparison between square-structured and triangle-structured PCF.

3.4. The chromatic dispersion property

The chromatic dispersion D is deduced using the following formula

$$D=-\frac{\lambda}{c}\frac{d^2 n_{eff}}{d\lambda^2} \tag{6}$$

Where n_{eff} is the effective index of the fundamental mode; c is the velocity of light in a vacuum. The chromatic dispersion takes into consideration the effects of both the material dispersion and the guide dispersion. Fig. 8 presents the chromatic dispersion of two PCFs with d= 0.46 μm, 0.8 μm and A=2.3 μm. Chromatic dispersion could be controlled by varying the hole diameter (or hole-to-hole spacing), which indicates the potentiality of applying the PCFs to optical communication systems, dispersion compensation, and nonlinear optics.

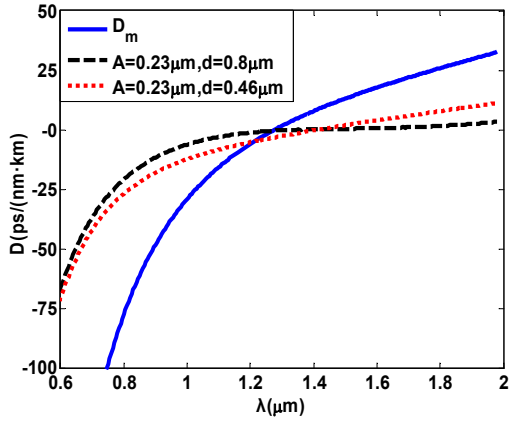

Fig. 8. Chromatic dispersion versus wavelength for PCFs with d= 0.46 μm, 0.8 μm and A=2.3 μm.

4. Conclusion

In this paper, we have presented a modified localized orthogonal function method to calculate accurately the square-structured PCFs. Extensive numerical simulations of PCFs such as endlessly single mode operation, electric field distribution, effective areas and chromatic dispersion property with varying air hole size or hole-to-hole spacing are investigated. It is supposed that the results discussed in this paper will have a significant impact on many engineering applications using PCFs.

Acknowledgement

This work was supported by the National Natural Science Foundation of China (Grant No.60671036 and No.60637010).

Reference

[1] T. A. Birks, J. C. Knight, P. St. J. Russell, Opt. Lett. **22**, 961 (1997).
[2] N. A. Mortensen , Opt. Express **10**, 341 (2002).
[3] J. C. Knight, J. Arriaga, T. A. Birks, IEEE Photonics Techn. Lett, **12**, 807 (2000).
[4] A. Ortigosa-Blanch, J. C. Knight, W. J. Wadsworth, Opt. Lett, **25**, 1325 (2000).
[5] Stig Barko Libori, Jes Broeng, Erik Knudsen OFC 2001[C].
[6] J. C. Knight, J. Broeng, T. A. Birks, P. St. J. Russell, Science. **282**, 1476 (1998).
[7] R. F. Cregan, B. J. Mangan, J. C. Knight, T. A. Birks, P. St. J. Russell, D. C. Allan, Science. **285**, 1537 (1999).
[8] J. C. Knigh, T. A. Birks, P. St. J. Russell, D. M. Atkin, Opt. Lett. **21**, 1547 (1996).
[9] A. Ferrando, E. Silvester, J. J. Miret, P. Andres, M. V. Andres, Opt. Lett. **24**, 276 (1999).
[10] A. Ferrando, E. Silvester, J. J. Miret, P. Andres, Opt. Soc. Amer. A **17**, 1333 (2000).
[11] T. M. Monro, D. J. Richardson, N. G. R. Broderick, J. Lightwave. Technol. **17**, 1093 (1999).
[12] Erik Knudsen, Anders Bjarklev, Optics Communications. **222**, 155 (2003).
[13] M. Qiu, Microw. Opt. Technol. Lett. **30**, 327 (2001).
[14] T. P. White, B. T. Kuhlmey, R. C. McPhedran, D. Maystre, G. Renversez, C. M. de Sterke, L. C. Botten, J. Opt. Soc. Amer. B. **19**, 2322 (2002).
[15] B. T. Kuhlmey, T. P. White, G. Renversez, D. Maystre, L. C. Botten, C. M. de Sterke, R. C. McPhedran, J. Opt. Soc. Amer. B. **19**, 2331 (2002).
[16] F. Fogli, L. Saccomandi, P. Bassi, Opt. Express. **10**, 54 (2002).
[17] F. Brechet, J. Marcou, D. Pagnoux, P. Roy, Opt. Fiber Technol. **6**, 181 (2000).
[18] M. Koshiba, K. Saitoh, Opt. Lett. **29**, 1739 (2004).
[19] G. Agrawal, Nonlinear Fiber Optics, 2nd. San Diego, CA:Academic ,1995.
[20] M. Mani Roja, IEEE (2006).

*Corresponding author: tx137@sohu.com